ALMA MATER STUDIORUM
UNIVERSITÀ DI BOLOGNA

ARCHIVIO ISTITUZIONALE
DELLA RICERCA

Alma Mater Studiorum Università di Bologna
Archivio istituzionale della ricerca

Macrocyclic naphthalene diimides as G-quadruplex binders

This is the final peer-reviewed author's accepted manuscript (postprint) of the following publication:

Published Version:
Marchetti, C., Minarini, A., Tumiatti, V., Moraca, F., Parrotta, L., Alcaro, S., et al. (2015). Macrocyclic naphthalene diimides as G-quadruplex binders. BIOORGANIC & MEDICINAL CHEMISTRY, 23(13), 3819-3830 [10.1016/j.bmc.2015.03.076].

Availability:
This version is available at: https://hdl.handle.net/11585/516279 since: 2020-02-14

Published:
DOI: http://doi.org/10.1016/j.bmc.2015.03.076

Terms of use:

Some rights reserved. The terms and conditions for the reuse of this version of the manuscript are specified in the publishing policy. For all terms of use and more information see the publisher's website.

This item was downloaded from IRIS Università di Bologna (https://cris.unibo.it/).
When citing, please refer to the published version.

(Article begins on next page)

12 October 2024

This is the final peer-reviewed accepted manuscript of:

Marchetti, C.; Minarini, A.; Tumiatti, V.; Moraca, F.; Parrotta, L.; Alcaro, S.; Rigo, R.; Sissi, C.; Gunaratnam, M.; Ohnmacht, S. A.; Neidle, S.; Milelli, A. Macrocyclic Naphthalene Diimides as G-Quadruplex Binders. *Bioorganic & Medicinal Chemistry* **2015**, *23* (13), 3819–3830. https://doi.org/10.1016/j.bmc.2015.03.076.

The final published version is available online at:

https://doi.org/10.1016/j.bmc.2015.03.076

Rights / License:

The terms and conditions for the reuse of this version of the manuscript are specified in the publishing policy. For all terms of use and more information see the publisher's website.

This item was downloaded from IRIS Università di Bologna (https://cris.unibo.it/)

When citing, please refer to the published version.

Macrocyclic Naphthalene Diimides as G-Quadruplex Binders

Chiara Marchetti[a,d], Andrea Milelli[b*], Anna Minarini[a], Federica Moraca[c], Lucia Parrotta[c], Stefano Alcaro[c], Mekala Gunaratnam[d], Stephan A Ohnmacht[d], Stephen Neidle[d], Vincenzo Tumiatti[b]

[a]*Department of Pharmacy and Biotechnology, University of Bologna, 40126 Bologna, Italy*

[b]*Department for Life Quality Studies, University of Bologna, Rimini campus, 47921 Rimini, Italy*

[c]*Dipartimento di Scienze della Salute, Univerisità "Magna Græcia" di Catanzaro, Viale Europa, 88100, Catanzaro, Italy*

[d]*School of Pharmacy, University College London, London WC1N 1AX, UK*

Graphical abstract

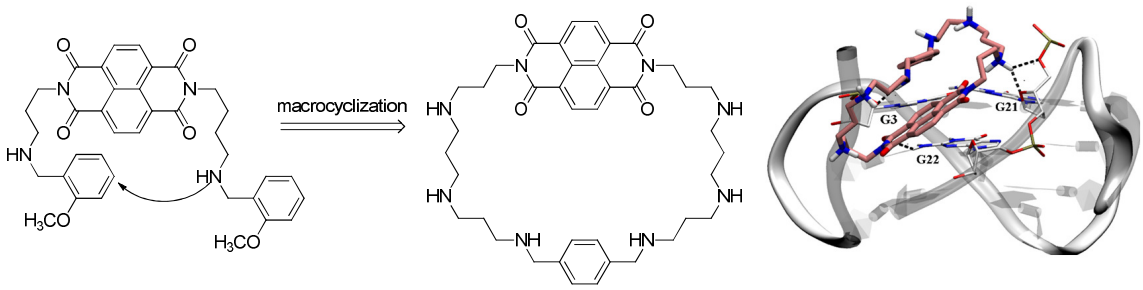

Abstract

The synthesis, biological and molecular modeling evaluation of a series of macrocyclic naphthalene diimides is reported. The present investigation expands on the study of structure-activity relationships of prototype compound **2** by constraining the molecule into a macrocyclic structure with the aim of improving its G-quadruplex binding activity and selectivity. The new derivatives, compounds **4-7** carry spermidine- and spermine-like linkers while in compound **8** the inner basic nitrogen atoms of spermine have been replaced with oxygen atoms**.** The design strategy has led to potent compounds stabilizing both human telomeric (F21T) and c-KIT2 quadruplex sequences, and high selectivity for quadruplex in comparison to duplex DNA (Tloop). Antiproliferative effects of the new derivatives **4-8** have been evaluated in a panel of cancer cell lines and all the tested compounds showed activity in the low micromolar or sub-micromolar range of concentrations. In order to rationalize the molecular basis of the DNA G-quadruplex *versus* duplex recognition preference, conformational and docking studies have been performed. The computational results support the observation that the main driving force in the recognition is due to electrostatic factors.

* **Corresponding author:** Dr. Andrea Milelli, Department for Life Quality Studies, University of Bologna, C.so D'Augusto 237, 47921 Rimini, Italy; phone 390541434609; fax: +390541434608, andrea.milelli3@unibo.it

Keywords: G-quadruplex, Naphthalene Diimide, Telomeric DNA, c-kit, docking.

Abbreviations: Alternative Lengthening Mechanisms, ALT; Naphthalene diimides, NDI; Fluorescence Resonance Energy Transfer, FRET; sulforhodamine, SRB; Polyamines Transport Systems, PTS.

1. Introduction

DNA has and continues to be the foremost single target in anticancer drug therapy with a number of drugs currently used in therapy exerting their action by interacting with it.[1] The most common

conformation assumed by DNA is the double helix described by Watson and Crick but, in the last few years, other secondary structures endowed with relevant biological roles have been discovered, notably the G-quadruplex.[2] Guanine-rich DNA tracts can assemble into G-quadruplexes due to specific guanine:guanine association through Hoogsteen hydrogen bonds. Quadruplex-forming sequences are located in several distinct regions of the human genome such as oncogene promoters[3] and telomeric regions.[4] G-quadruplexes appear to play critical roles in a range of biological processes including telomere maintenance, replication and transcription. Telomeres are regions of G-rich highly-repetitive DNA sequences (-TTAGGG- in humans) located at the end of chromosomes, whose purpose is to provide protection against DNA degradation and unwanted recombination. In normal cells, DNA polymerase is unable to replicate the 3' ends of telomeric DNA repeats and telomere length is shortened after each replication cycle until a critical length is reached, leading to senescence or apoptotic cell death[5]. In transformed cells, this critical length is never reached due to the expression of the telomerase enzyme, which adds hexameric DNA sequence repeats 5´-TTAGGG-3´ to 3´ telomeric DNA ends. Hence, telomerase, by maintaining telomere length and integrity, plays a key role in ensuring the immortalized replication of cancer phenotypes[6]. Telomerase expression is very low in somatic cells but the enzyme is up-regulated in almost 80% of human cancers, including those of brain, skin, lung and blood, and represents a major anticancer target[7]. A range of approaches have been explored in order to block the biological activity of this enzyme[8] by means of vaccines (GV1001),[9] oligonucleotides (Imetelstat)[10], and small molecule inhibitors (BIBR1532).[11] Unfortunately, telomerase is a challenging target and clinical trials have had only moderate success to date.[12,13] Furthermore, a percentage of human cancer cells are telomerase-negative and may use Alternative Lengthening Mechanisms (ALT) to elongate telomeres.[14] An indirect approach to induce telomere shortening relies on the induction and stabilization of G-quadruplexes: the stabilization of these secondary structures at telomeric ends can result in the blockage of telomerase activity because of the lack of sufficient single stranded telomeric DNA. This approach has been validated by the demonstration that quadruplex arrangements inhibit telomerase activity *in vitro* and *in vivo*.[15,16] Recently, this concept has been further validated by Balasubramian and coworkers who reported direct visualization and small molecule-mediated stabilization of G-quadruplex structures in human cells.[17] Further, stabilization of G-quadruplexes located in promoter regions of oncogenes, such as c-KIT,[18] c-MYC,[19] k-RAS,[20] VEGF,[21] and hTERT[22] has been shown to result in down-regulation of the expression of these targeted genes.[3] It has been recently demonstrated that ALT-positive cells are sensitive to G-quadruplex ligands since the stabilization of these structures is able to prevent the execution of the first steps of the alternative elongation process.[23] These findings have boosted the interest in designing selective G-quadruplex stabilizing agents, also exploiting structural information obtained by crystallographic and NMR studies.[24,25,26] Several G-quadruplex binding molecules show promising anticancer activity either in cells or in tumor xenograft models and, among them, Quarfloxin has reached clinical trials.[27] Most of these compounds share common generic structural features as planar polycyclic hetero-aromatic cores and positively charged side chain(s); however, an increasing number of G-quadruplex binders lacking these features have been recently reported.[26] A number of macrocyclic compounds, such as telomestatin, have been shown to selectively bind G-quadruples sequences (Fig.1).[28] This natural product is very selective in stabilizing telomeric G-quadruplex over duplex DNA and shows promising anticancer activity both *in vitro* and *in vivo* models.[29] However, it has not been further developed mainly due to its unfavorable pharmacological properties. Telomestatin and, in general, macrocyclic compounds are particularly

interesting for G-quadruplex targeting for two main reasons: on one hand they show low affinity for duplex DNA since for steric reasons it is more difficult for them to intercalate between base pairs and, on the other, they adapt very well to stacking on the terminal G-quartet structure of the G-quadruplexes that is the site accessible to large-area planar aromatics. An example of how macrocycles represent an interesting opportunity for specifically G-quadruplex targeting derives from the compound BOQ1: this is a macrocyclic bis-quinacrine that binds G-quadruplex in a stronger and more specific way than the monomer MOQ2 (F21T stabilization ΔT_m in °C: BOQ1 = 28, MOQ2 = 10) (Fig.1).[30]

Naphthalene diimides (NDIs) represent an especially promising class of G-quadrupex binders and over the last few years a number of NDI-based compounds have been developed in part by exploiting the available NDI-G-quadruplex crystal structures.[31,32] Compound **1**, a tetrasubstituted NDI obtained through structure-based optimization of previously reported NDIs, shows high affinity towards human telomeric and HSP90 quadruplex sequences and is highly active towards pancreatic MIA-PaCa-2 and PANC-1 cell lines (Fig.1).[32]

Fig. 1. Selected examples of G-quadruplex binders.

We recently reported on the di-substituted NDI compound **2**, which has submicromolar antiproliferative activity in several cancer cell lines; this compound, bearing *o*-methoxybenzylamine side chains, strongly binds dsDNA (EC_{50} = 122 nM) and induces apoptotic cell death.[33] Further optimization studies led to discovery of **3**, the tri-methoxy substituted analogue of **2**, which has enhanced the cytotoxic activity in a number of cell lines (Fig.2).[34, 35] An important finding arose from studies of structure-activity relationships on this series of molecules was that growth-inhibitory activity and DNA-binding properties strongly depend on the number of positive charges, the length of the alkyl chains between the nitrogen atoms and the NDI scaffold and on the nature of the substituent on the aromatic rings.

As previously reported, a number of G-quadruplex binders are characterized by a macrocyclic structure; notwithstanding that the design of macrocycles is a well-established technique in medicinal chemistry to improve affinity and selectivity for a given biological target, macrocyclization has been underexploited mainly due to synthetic issues.[36] As reported for BOQ1 and its monomer MOQ2, macrocyclization can enhance biological properties of quadruplex-binding ligands since conformationally "locked" analogues of non-cyclic molecules can interact with the larger surface area that differentiates quadruplex from duplex nucleic acids.

On this basis, the aim of the present investigation is to expand structure-activity relationships of **2**, by constraining the molecule into a macrocyclic structure to improve its G-quadruplex binding activity and selectivity. To this end macrocyclic NDIs **4-8** have been designed by locking the flexible chains of **2** through a phenyl ring (Fig.2). Since the presence of positive charges in the side chains is a requirement for the interaction with G-quadruplex,[37] we decided to increase the number of nitrogen atoms, protonated at physiological pH, in order to establish additional interaction with the target. In particular, compound **4** is characterized by side-chains derived from nor-spermidine,

while **7** contains side chains derived from spermine. With the aim of evaluating the importance of the width of the macrocycle for its interaction with G-quadruplex, compounds **5** and **6**, characterized by a spermine-like side chains differing in the length of the spacer between the inner nitrogen atoms, were synthesized. Finally, in order to investigate the role of positively charged nitrogen atoms, we designed compound **8** where the two inner nitrogen atoms of **7** have been replaced with oxygen atoms: indeed, oxygen, like nitrogen, can establish hydrogen bonds with a biological counterpart but it is not able to form ionic interactions. During the drafting of this manuscript, Takenaka and coworkers reported on cyclic NDI derivatives pointing out their ability to bind to different DNA structures[38, 39]. Their results strengthened the rationale of the present investigation, and we have explored and expanded the same approach.

Fig.2. Drug Design Strategy leading to **4-8**.

2. Results and Discussion

2.1 *Chemistry*

Target compounds **4-8** have been synthesized following the procedure depicted in Scheme 1 and characterized by ^{1}H-NMR, ^{13}C-NMR and Mass Spectroscopy. The suitable Boc-protected triamine **9** and diBoc-protected tetramines **10-12**[40] were selectively protected at one of the two basic functions through reaction with ethyl trifluoroacetate leading to **14-17**, while commercially available 4,9-dioxa-1,12-dodecanediamine **13** was reacted with Boc_2O to obtain the corresponding mono-amine **18**. These resulting intermediates were condensed with naphthalene-tetracarboxylic dianhydride to provide **19-23**. Basic hydrolysis of the trifluoro-acetyl protecting group led to diamine **24-27** while removal of the Boc protecting group was achieved through acidic hydrolysis giving **28**. Macrocyclization was obtained through a one-step synthetic protocol that includes condensation of the primary amine groups of the adducts **24-28** with terephthalaldehyde, followed by reduction of the Schiff base formed with $NaBH_4$, leading to the intermediate macrocycle **29-32** and the target macrocycle **8**. Slow dropwise addition of the dialdehyde within 72 h and high dilution conditions are critical for the success of the cyclization step. Boc-deprotection of **29-32** led to the final products **4-7**. All the target compounds were transformed to hydrochloride salts in order to obtain derivatives that are easier to handle.

Scheme 1.

2.2 *Biological investigations*

Target compounds **4-8** have been firstly evaluated for their ability to stabilize G-quadrupex sequences. FRET (Fluorescence Resonance Energy Transfer) melting experiments on human telomeric (F21T) and on c-KIT2 promoter quadruplex sequences have been performed. Since one of the most important goal in the design of G-quadruplex binders relies in achieving high selectivity towards G-quadruplexes over double-stranded DNA, to this end melting data obtained with a

duplex DNA sequence (T loop) are reported (Table 1). All three sequences contained the FAM/TAMRA donor/acceptor combination. All compounds have been evaluated at 1 μM concentration. It appears that macrocyclization leads to an increase in G-quadruplex stabilization for all the new compounds, with the exception of **8**. The most effective binder for the human telomeric F21T G-quadruplex sequence is **7,** characterized by side chains derived from spermine (3-4-3). **7** gives a ΔT_m value of 26.8 °C at 1 μM (ΔT_m = 31.9 °C at 2 μM, not reported), a much higher value than that obtained with the starting compound **2** (ΔT_m = 9.9 °C at 1 μM). Closely related to **7**, compounds **5** and **6** are characterized by a shorter spermine-like side chains differing by the number of methylene groups separating the two inner nitrogen atoms. In this series, stabilization of G-quadruplexes is higher when the linker separating the two inner nitrogen atoms is four methylene groups, as in **7**, and decrease by reducing the number of methylene to three (**6**, ΔT_m = 22.1 °C at 1 μM) and two (**5**, ΔT_m = 18.9 °C at 1 μM). It is notable that replacement of the inner nitrogen of **7** with oxygen atoms (**8**) abolishes the DNA-binding ability (ΔT_m = 0.4 °C): this finding suggests that **7**, likely due to its ionized state higher than **8**, can establish with the DNA stronger electrostatic interactions. Elimination of two nitrogen atoms from **7** leads to **4** which shows far less stabilization for G-quadruplexes (ΔT_m = 12.6 °C at 1 μM) underlying the requirement of nitrogen atoms for good interactions with the target. From the dsDNA data, it emerges that affinity follows the same pattern observed towards G-quadruplex sequences: compound **7** shows the highest stabilisation (ΔT_m = 8.6 °C) followed by **6** (ΔT_m = 3.3 °C) and **5** (ΔT_m = 1.2 °C). Also in this case, removal of two nitrogen atoms leads to a decrease in stabilization (**4**, ΔT_m = 1.4 °C) and the replacement of the nitrogen atoms with oxygens almost abolishes the interaction. As already mentioned, G-quadruplex binders can hinder the transcription of, for example, human oncogenes, by binding to the quadruplex sequences located in their promoter regions.. c-KIT is an important oncogene encoding for the KIT tyrosine kinase receptor and represents an attractive target in the treatment of gastrointestinal tumors. Two quadruplex sequences (c-KIT1 and c-KIT2) in the kit promoter have been identified[41,18] and, recently, Gunaratnam et al. have reported a NDI-based derivative able to stabilize the c-KIT2 quadruplex with significantly higher ΔT_m values respect to c-KIT1.[42] For this reason, we also decided to evaluate our NDI-based macrocycles with the c-KIT2 G-quadruplex sequence. Gratifyingly, all of the tested compounds, again with the exception of **8**, show a significant stabilizing effect on the c-KIT2 quadruplex. In particular, **7** shows highest stabilizing activity (ΔT_m = 33.1 °C at 1 μM, ΔT_m = 39.9 °C at 2 μM) while a linear decrease of stabilization was observed, again, by reducing the length of the chain between the two inner nitrogen atoms, eliminating one nitrogen atom from each side chain and replacing the nitrogen with oxygen atoms (**8**, ΔT_m = 0 °C at 1 μM).

Table 1

6 emerges as the most interesting compound of the group since it has the more balanced profile relative to both G-quadruplex and duplex stabilization.

As shown in Fig. 3, the FRET melting curve for compound **6** with the F21T and c-KIT2 quadruplex sequences at all the concentration tested (0.1-5 μM), shows a significant increase in melting

temperature for both the targets, especially at higher concentrations (4 and 5 μM). The compound is able to induce a ΔT_m value of around 40 °C, which is the maximum that can be measured by the assay, thus confirming its optimal quadruplex targeting profile.

Fig.3

To investigate the telomerase inhibitory activity of the macrocyclic derivative **6** was tested in MIA-PaCa-2 cells, using the modified TRAP-LIG assay (Fig1 SI). This compound does not display any activity against telomerase, with no change in the products of telomerase-mediated telomere elongation being apparent up to 50 μM ligand concentration. This finding agrees with previous reports that some NDI derivatives lack telomerase inhibitory activity, despite their ability to induce large increases in T_m (for F21T).[31]

All the newly synthesized compounds were evaluated for their antiproliferative activity in a 96h sulforhodamine (SRB) assay in a panel of cancer cell lines (lung A549, breast MCF7, pancreatic MIA-PaCa-2 / PANC-1, Alternative Lengthening of Telomeres ALT) and human fibroblast (WI38). As reported in Table 2, compounds **4-8** display antiproliferative activity in a submicro- and micro-molar range. All compounds are less active than the reference compound **2**. Further, the activity seems to follow an inverse pattern compared with the result obtained in the *in vitro* assays. In particular, taking into account the spermine- and spermidine-derived compounds, the least effective G-quadruplex stabilizing agent **4** is the most active in cell-based assays, with an IC_{50} value in submicrolar- or low micromolar ranges in all five cancer cell lines, albeit with no cell-type selectivity. On the other hand, the most quadruplex-stabilising compound, **7,** in the *in vitro* assays is the least active in cell-based assays. It is notable that these compounds show antiproliferative activity in the ALT-positive cell line. This is in accord with the previously reported activity of some G-quadruplex binders in a telomerase-negative cell line.[23] The cellular activities of these new macrocyclic NDIs towards the normal fibroblast line are significantly less than that of the lead compound **2**, which is able to affect normal fibroblast cells.

Table 2.

In general, the antiproliferative effects appear to be unrelated to ΔT_m values for G-quadruplex stabilization. In particular, an inverse correlation between ΔT_m and IC_{50} values emerges: the most potent telomeric G-quadruplex binder **7** is the less active compound in all our panel of cancer cell lines, while the less stabilizing compound **8** is the most active agent in cells. Further, elimination of a nitrogen atom from each side chain, for instance from **7** leading to **4**, in spite of a pronounced decrease in ΔT_m, is accompanied by a marked increase of activity. A possible explanation of the non-correlated activity could be related to the different and unfavorable physicochemical properties of these compounds. Indeed, many G-quadruplex-binders do not have favorable drug-like properties (i.e. molecular weight, etc). Highly charged molecules, such as protonated polyamine-based compounds, may not have difficulty in crossing the cellular lipid bilayers since they could exploit an active Polyamines Transport System (PTS) to enter the cells,[43] although macrocyclic-polyamine PTS-mediated transport has not been reported to date.[44] We suggest that **4**, despite being the poorest

quadruplex binder, has greater cell growth inhibitory activity in cell panel in comparison to its higher homologues on the basis of its potentially superior pharmacological profile. We cannot discount the possibility that the observed cellular effects may not be G-quadruplex-mediated but derived from quite distinct mechanisms, although it may be that other DNA or RNA quadruplexes, which we have not evaluated, could be involved. It is well-established that polyamine-based compounds are able to interact with a multitude of biochemical targets[45-47] and exert cytotoxic activity through several mechanisms[48, 49]: macrocyclic-polyamine have been reported to display toxic effects by, for instance, depleting cellular ATP and interfering with enzymes involved in the polyamine biosynthetic pathway.[50] The possibility of multiple mechanisms of action is further suggested by the observation that **8** is the most active compound in the cancer cell lines tested despite its almost complete lack of DNA-binding activity; this result deserves further investigation.

2.3 Computational studies

*2.3.1 Receptor pre-treatment and molecular modelling of **6***

Docking calculations have been performed using X-Ray experimental models of a 6 bp DNA duplex (PDB code: 1Z3F) complexed with the anticancer agent ellipticine,[51] and the h-Tel sequence of the bimolecular quadruplex d(TAGGGTTAGGGT) (PDB code: 3CDM) co-crystallized with a tetra-substituted naphthalene-diimide,[52] in order to investigate the G-quadruplex vs duplex DNA selectivity of the lead compound **6** and provide a molecular description of its binding mode. Both these PDB models have been successfully employed in a previously reported study.[34] Before performing docking calculations, duplex and G-quadruplex PDB entries have been prepared by eliminating non-nucleic acid components, such as ligands, counter-ions and water molecules, included in the original experimental structures. For the 3CDM structure, based on two G-quadruplex subunits, only the most stable Chain B has been considered for the docking. The 3D molecular structure of compound **6** was built using the Maestro GUI interface ver. 9.7.[53] In order to take into account the experimental conditions, its protonation state at physiological pH (7.4) has been computed with LigPrep ver. 2.9,[54] revealing the ionization of the four aliphatic secondary amine groups of the spermine-like chain. The conformational degrees of freedom of **6** was first explored using our previous methodology for NDI derivatives.[55, 56] 3000 conformations were generated by means of the Monte Carlo method, using the AMBER* force field and the GB/SA water implicit solvent model, followed by energy minimization with the PRCG algorithm[57]. 56 conformers were found within 5 kcal/mol above the global minimum. Fig. 4 shows the potential energy (*kcal/mol*) calculated for each conformer.

Fig. 4

2.3.2 Docking results

The energetically most stable conformer of **6**, shown in Fig.4, ($E_{potential}$ = -238.672 kcal/mol) was used for docking calculations with the AutoDock 4.2 (AD4) software package,[58] which was

successfully used recently to target a DNA G-quadruplex with cyclic compounds.[59] With this aim, ligand and both duplex and quadruplex receptors were firstly converted to AD4 file format and Gaisteiger-Marsili partial charges were then assigned. In order to explore more of the conformational space of both nucleic acids, the box dimensions were defined to include the entire DNA molecules. 256 docking poses were generated. Finally, the complexes obtained were subjected to 5000 iterations of fully relaxed optimization with the same force-field and solvation model as used in the conformational search of **6**. The free energy of complexation was calculated and split for each non-bonding terms. For the duplex DNA (PDB code: 1Z3F), the lowest-energy bound conformation of **6** (ΔG = -27.18 *kcal/mol*) was located in the DNA minor groove (Fig. 5.A). The steric hindrance of the spermine-like side chains, prevents intercalation within the guanine-cytosine region and they are mostly involved in electrostatic interactions with the negatively-charged phosphate backbone as reported numerically in Table 3 and graphically in the Poisson-Boltzmann electrostatic potential surface area (Fig. 5.B). In addition, the formation of 2 H-bond interactions with the C5 residue contributes to the binding affinity.

Table 3

Fig. 5

Surprisingly, in the case of the human telomeric DNA quadruplex (PDB entry: 3CDM), although the *top* and *bottom* areas of the G-tetrads are well suitable for π-π stacking interactions with the NDI core, the most energetically stable (ΔG = -63.69 *kcal/mol*) and populated (with a Boltzmann probability of 98.95%) conformation of **6** is in a groove, close to the G21:G3:G22 residues (Fig. 6.A). This finding confirms that, due to the four positively-charged nitrogen atoms, the major driving force in the binding process of **6** is the electrostatic term. This observation is supported numerically (Table 3) and shown graphically in Fig. 6.B. These results indicate only minor contributions of van der Waals and H-bond terms, although adding to improved G-quadruplex recognition. The solvation term GB/SA is the only one favoring duplex recognition, but this is due to the different net number of charges considered in the nucleic acid models.

Fig. 6

The same computational protocol has been used to model the interaction of **8** against both targets (Fig. 2SI and Table 1SI). In agreement with experimental data, we found that the different ionization state influences its DNA recognition with respect to compound **6**. This is mostly due to the minor electrostatic contribution of **8** and also to the reduction of the hydrogen bond network, due to the presence of only two protonable nitrogen atoms.

3. Conclusion

In summary, with the aim of expanding the structure-activity relationship studies of compound **2,** a series of macrocyclic NDIs **4-8** have been synthesized. Such derivatives bear, spermidine- and spermine-like side chains varying in the length between the inner nitrogen atoms, with the exception of **8**. The new compounds show increased stabilization of both human telomeric (F21T) and c-KIT2 quadruplex sequences and have some selectivity over duplex DNA (using the Tloop sequence), confirming the robustness of the design. Molecular modeling studies have been performed and, in agreement with experimental data, compound **6** was found to be highly selective for a DNA G-quadruplex topology with respect to duplex DNA. A further evaluation of the non-covalent bond interactions has shown that the protonated four aliphatic secondary amine groups of the spermine-like side chains are the most involved moiety of the designed macrocyclic NDI in quadruplex recognition. Hence, the electrostatic component is the main driving force in the binding process although even H-bond interactions can play a role in quadruplex/duplex selectivity. These compounds also show significant cell growth inhibition activity in sub- to micro-molar concentration ranges in a panel of cancer cell lines. This activity does not obviously correlate with the observed *in vitro* data, possibly because of unfavorable physicochemical profiles of these molecules, or possibility because of other mechanisms of actions. Despite this, the respectable *in vitro* and cellular activity suggests that appropriate modifications to improve drug-like features could result in enhanced biological profiles. Further biological investigations of these derivatives and synthesis of new compounds are currently ongoing in our laboratory and results will be reported in due course.

Experimental Section

Uncorrected melting point was taken in glass capillary tubes on a Buchi SMP-20 apparatus. ESI-MS spectra were recorded on Perkin Elmer 297 and Waters ZQ 4000. ^{1}H-NMR and ^{13}C-NMR were recorded on Varian VRX 200 and 400 instruments. Chemical shifts are reported in parts per million (ppm) relative to peak of tetramethylsilane (TMS) and spin multiplicities are given as s (singlet), br s (broad singlet), d (doublet), t (triplet), q (quartet) or m (multiplet). Chromatographic separations were performed on silica gel columns by flash (Kieselgel 40, 0.040 e 0.063 mm, Merck) column chromatography. Reactions were followed by thin layer chromatography (TLC) on Merck (0.25 mm) glass-packed pre-coated silica gel plates (60 F254) and then visualized in an iodine chamber or with a UV lamp.

General procedure for the synthesis of 14-17.

The appropriate compound **9-12** (3 eq) was dissolved in MeOH at 0°C and ethyl trifluoroacetate (1 eq) was added dropwise. The solution was allowed to stir for 16 h at room temperature, then the reaction mixture was evaporated and the residue was purified by flash chromatography eluting with a mixture of CH_2Cl_2/MeOH/33% aq.NH_4OH 9/1/0.1 to give **14-17**.

tert-butyl (3-aminopropyl)(3-(2,2,2-trifluoroacetamido)propyl)carbamate (14): Yellow oil: 95% yield; ^{1}H NMR (400MHz, $CDCl_3$) δ 1.41-1.44 (s, 9H), 1.63-1.68 (m 4H), 1.75 (brs, 2H, exch D_2O), 3.20 (t, 2H, *J* = 6 Hz), 3.28-3.29 (m, 4H), 3.42-3.47 (m, 2H), 8.17 (brs, 1H, exch D_2O). MS (ESI) *m/z* = 328 $(M+H)^+$

tert-butyl (3-aminopropyl)(2-((tert-butoxycarbonyl)(3-(2,2,2-trifluoroacetamido) propyl)amino)ethyl)carbamate (15): Yellow oil: 93% yield; ^{1}H NMR (400MHz, $CDCl_3$) δ 1.42-

1.43 (s, 18H), 1.61-1.68 (m, 4H), 1.77 (brs, 2H, exch D_2O), 2.66 (t, 2H, *J* = 6.0 Hz), 3.23-3.26 (m, 10H), 8.12 (brs, 1H, exch D_2O). MS (ESI) *m/z* = 471 $(M+H)^+$

tert-butyl (3-aminopropyl)(3-((tert-butoxycarbonyl)(3-(2,2,2-trifluoroacetamido) propyl)amino)propyl)carbamate (16): Yellow oil: 83% yield; ^{1}H NMR (400MHz, $CDCl_3$) δ 1.44-1.45 (s, 18H), 1.65-1.76 (m, 6H), 1.94 (brs, 2H, exch D_2O), 2.70 (t, 2H, *J* = 6 Hz), 3.13-3.19 (m, 4H), 3.29-3.36 (m, 6H), 8.15 (brs, 1H, exch D_2O). MS (ESI) *m/z* = 485 $(M+H)^+$

tert-butyl(3-aminopropyl)(4-((tert-butoxycarbonyl)(3-(2,2,2trifluoroacetamido) propyl)amino)butyl)carbamate (17): Yellow oil: 74% yield; ^{1}H NMR (200MHz, $CDCl_3$) δ 1.34-1.59 (s, 18H), 1.60-1.81 (m, 6H), 2.65-2.85 (m, 2H), 2.86-3.08 (m, 2H), 3.08-3.40 (m, 10H). MS (ESI) *m/z* = 499 $(M+H)^+$

Synthesis of tert-butyl (3-(4-(3-aminopropoxy)butoxy)propyl)carbamate (18): 4,9-dioxa-1,12-dodecanediamine **13** (10 eq) was dissolved in CH_2Cl_2 (15 ml), a solution of Boc_2O (1 eq) in CH_2Cl_2 was slowly added dropwise. The reaction mixture was stirred at room temperature for 16 h and after the solvent was removed under vacuum, the residue was taken up with H_2O (15 ml) and extracted with CH_2Cl_2 (3x15 ml). The organic phase was dried over Na_2SO_4 and the solvent removed to obtain **18**. Yellow oil: 93% yield; ^{1}H-NMR (400 MHz) δ 1.44 (s, 9H), 1.62-1.77 (m, 8H), 2.77-2.81 (m, 2H), 3.20-3.21 (m, 2H), 3.40-3.50 (m, 8H), 5.21 (brs, 1H, exch D_2O). MS (ESI) *m/z* = 305 $(M+H)^+$

General procedure for the synthesis of 19-23.

To a solution of **14-18** (2 eq) in DMF was added 1,4,5,8-Naphthalentetracarboxylicdianhydride (1 eq) and the mixture was refluxed until the starting material was consumed (about 2 h). Following solvent removal, the residue was purified by flash chromatography eluting with a mixture of petroleum ether/ethyl acetate 5/5 to give the desired compounds **19-23**.

di-tert-butyl((1,3,6,8-tetraoxobenzo[lmn][3,8]phenanthroline-2,7(1H,3H,6H,8H)-diyl)bis(propane-3,1-diyl))bis((3-(2,2,2-trifluoroacetamido)propyl)carbamate) (19): Yellow oil: 47% yield; ^{1}H NMR (400MHz, $CDCl_3$) δ 1.44 (s, 18H), 1.74-1.78 (m, 4H), 1.96-2.03 (m, 4H), 3.35-3.37 (m, 12H), 4.20 (t, 4H, *J* = 8.0 Hz), 8.13 (brs, 2H, exch D_2O), 8.76 (s, 4H). MS (ESI) *m/z* = 887 $(M+H)^+$

di-tert-butyl((1,3,6,8-tetraoxobenzo[lmn][3,8]phenanthroline-2,7(1H,3H,6H,8H)-diyl)bis(propane-3,1-diyl))bis((2-(3,3-dimethyl-N-(3-(2,2,2trifluoroacetamido)propyl)butanamido)ethyl)carbamate) (20): Brown oil: 16% yield; ^{1}H NMR (400MHz, $CDCl_3$) δ 1.41-1.44 (m, 36H), 1.70-1.76 (m, 4H), 1.97-2.01 (m, 4H), 3.24-3.31 (m, 20H), 4.18-4.20 (m, 4H), 8.42 (brs, 2H, exch D_2O), 8.74 (s, 4H). MS (ESI) *m/z* = 1069 $(M+H)^+$

di-tert-butyl((1,3,6,8-tetraoxobenzo[lmn][3,8]phenanthroline-2,7(1H,3H,6H,8H)-diyl)bis(propane-3,1-diyl))bis((3-((tert-butoxycarbonyl)(3-(2,2,2-trifluoroacetamido)propyl)amino)propyl)carbamate) (21): Brown oil: 43% yield; ^{1}H NMR (400MHz, $CDCl_3$) δ 1.30-1.40 (m, 36H), 1.64-1.69 (m, 4H), 1.71-1.74 (m, 4H), 1.89-1.94 (m, 4H), 3.10-3.25 (m, 20H), 4.12 (t, 4H, *J* = 8.0 Hz), 8.11 (brs, 2H, exch D_2O), 8.66 (s, 4H). MS (ESI) *m/z* = 1201 $(M+H)^+$

di-tert-butyl((1,3,6,8-tetraoxobenzo[lmn][3,8]phenanthroline-2,7(1H,3H,6H,8H)-diyl)bis(propane-3,1-diyl))bis((4-((tert-butoxycarbonyl)(3-(2,2,2-trifluoroacetamido)propyl)amino)butyl)carbamate) (22): Brown oil: 50% yield; ^{1}H NMR

(400MHz, $CDCl_3$) δ 1.24-1.44 (m, 36H), 1.45-1.51 (m, 8H), 1.67-1.70 (m, 4H), 1.96-1.99 (m, 4H), 3.15-3.18 (m, 4H), 3.24-3.30 (m, 16H), 4.19-4.21 (m, 4H), 8.02 (brs, 2H, exch D_2O), 8.74 (s, 4H). MS (ESI) *m/z* = 1229 $(M+H)^+$

di-tert-butyl((((((1,3,6,8-tetraoxobenzo[lmn][3,8]phenanthroline-2,7(1H,3H,6H,8H)-diyl)bis(propane-3,1-diyl))bis(oxy))bis(butane-4,1-diyl))bis(oxy))bis(propane-3,1-diyl))dicarbamate (23): Brown oil: 90% yield; ^1H NMR (400MHz, $CDCl_3$) δ 1.41 (s, 18H), 1.52-1.54 (m, 4H), 1.69-1.72 (m, 8H), 1.99-2.03 (m, 4H), 3.17-3.18 (m, 4H), 3.31-3.34 (m, 4H), 3.38-3.44 (m, 8H), 3.52-3.55 (m, 4H), 4.29 (t, 4H, *J* = 6.0 Hz), 4.90 (brs, 2H, exch D_2O), 8.71 (s, 4H). MS (ESI) *m/z* = 841 $(M+H)^+$

General procedure for the synthesis of 24-27.

The appropriate compound **19-22** (1 eq) was dissolved in a mixture of MeOH/H_2O (10:1 ratio, 20 ml) and to the resulting solution was added K_2CO_3 (10 eq). The reaction mixture was refluxed for 2 h, then the solvent was removed and the residue was taken up with H_2O (15ml) and extracted with CH_2Cl_2 (3x10ml). The organic phase was dried over Na_2SO_4, evaporated in vacuo and the residue was purified by flash chromatography eluting with a mixture of CH_2Cl_2/MeOH/33% aq.NH_4OH 8/2/0.2 to give **24-27**.

di-tert-butyl((1,3,6,8-tetraoxobenzo[lmn][3,8]phenanthroline-2,7(1H,3H,6H,8H)-diyl)bis(propane-3,1-diyl))bis((3-aminopropyl)carbamate) (24): Yellow oil: 60% yield; ^1H NMR (400MHz, $CDCl_3$) δ 1.42 (s, 18H), 1.62-1.80 (m, 4H), 1.95-1.99 (m, 4H), 2.77-2.80 (m, 4H), 3.13-3.29 (m, 8H), 4.16-4.21 (m, 4H), 8.72 (s, 4H). MS (ESI) *m/z* = 695 $(M+H)^+$

di-tert-butyl((1,3,6,8-tetraoxobenzo[lmn][3,8]phenanthroline-2,7(1H,3H,6H,8H)-diyl)bis(propane-3,1-diyl))bis((2-((3-aminopropyl)(tert-butoxycarbonyl)amino)ethyl)carbamate) (25): Brown oil: 44% yield; ^1H NMR (400MHz, $CDCl_3$) δ 1.49 (s, 36H), 1.72-1.90 (m, 4H), 1.96-2.00 (m, 4H), 3.68-3.87 (m, 4H), 3.32-3.33 (m, 16H), 4.21-4.25 (m, 4H), 8.75 (s, 4H). MS (ESI) *m/z* = 981 $(M+H)^+$

di-tert-butyl((1,3,6,8-tetraoxobenzo[lmn][3,8]phenanthroline-2,7(1H,3H,6H,8H)-diyl)bis(propane-3,1-diyl))bis((3-((3-aminopropyl)(tert-butoxycarbonyl)amino)propyl)carbamate) (26): Brown oil: 63% yield; ^1H NMR (400MHz, $CDCl_3$) δ 1.42-1.44 (m, 36H), 1.79-1.81 (m, 8H), 1.96-1.97 (m, 4H), 2.87-2,94 (m, 4H), 3.16-3.23 (m, 8H), 3.24-3.33 (m, 8H), 4.20 (t, 4H, *J* = 8.0 Hz), 8.76 (s, 4H). MS (ESI) *m/z* = 1009 $(M+H)^+$

di-tert-butyl((1,3,6,8-tetraoxobenzo[lmn][3,8]phenanthroline-2,7(1H,3H,6H,8H)-diyl)bis(propane-3,1-diyl))bis((4-((3-aminopropyl)(tert-butoxycarbonyl)amino)butyl)carbamate) (27): Brown oil: 61% yield; ^1H NMR (400MHz, $CDCl_3$) δ 1.37-1.40 (m, 36H), 1.44-1.49 (m, 12H), 1.95-2.01 (m, 4H), 2.93-3.01 (m, 4H), 3.20-3.51 (m, 16H), 4.18 (m, 4H), 8.83 (s, 4H). MS (ESI) *m/z* = 1037 $(M+H)^+$

2,7-bis(3-(4-(3-aminopropoxy)butoxy)propyl)benzo[lmn][3,8]phenanthroline-1,3,6,8(2H,7H)-tetraone (28): To a stirring solution of **23** (1 eq) in MeOH (10 ml), HCl 3N (10 ml) was added dropwise at 0° C. The stirring was continued for 16 h. The solvent was removed, the residue was taken up with H_2O (10 ml) and washed with Et_2O; the aqueous phase was basified with NaOH and this solution was extracted with CH_2Cl_2 (3x10 ml). The organic phase was dried over Na_2SO_4 to obtain the desire product **28**. Yellow oil: 88% yield; ^1H NMR (400MHz, $CDCl_3$) δ 1.48-1.51 (m, 8H), 1.71-1.73 (m, 4H), 2.00-2.03 (m, 4H), 2.81-2.83 (m, 4H), 3.31 (t, 4H, *J* = 5.8 Hz), 3.37 (t, 4H,

J = 5.8 Hz), 3.44 (t, 4H, *J* = 6.4 Hz), 3.54 (m, 4H, *J* = 6.0 Hz), 4.30 (t, 4H, *J* = 7.0 Hz), 8.74 (s, 4H). MS (ESI) *m/z* = 641 $(M+H)^+$

General procedure for the synthesis of 29-32 and 8. The appropriate precursor **24-28** (1 eq) was dissolved in EtOH (50 ml of solvent / 1 mmol of amine) and 3Å molecular sieves were added to the solution. A solution of terephthalaldehyde (1eq) in EtOH (50 ml of solvent / 1mmol of aldehyde) was added dropwise within 72 h. Then $NaBH_4$ (1eq) was added to the solution and the stirring was continued for 16 h at room temperature. The solvent was evaporated, the residue was taken up with CH_2Cl_2 and washed with brine. The organic phase was dried and evaporated in vacuo, the residue was purified by flash chromatography eluting with a mixture of CH_2Cl_2/MeOH/33% aq.NH_4OH 9/1/0.03 to give **29-32** and **8**. **8** was then dissolved in Et_2O and treated with Et_2O saturated with HCl, in order to obtain **8** as the dihydrochloride salt.

(29): Yellow oil: 26% yield; ^{1}H NMR (400MHz, $CDCl_3$) δ 1.39-1.48 (m, 22H), 2.00-2.03 (m, 4H), 2.44-2.49 (m, 4H), 3.14-3.17 (m, 4H), 3.25-3.29 (m, 4H), 4.09 (s, 4H), 4.27-4.31 (m, 4H), 6.94 (s, 4H), 8.71 (s, 4H). MS (ESI) *m/z* = 797 $(M+H)^+$

(30): Yellow oil: 31% yield; ^{1}H NMR (400MHz, $CDCl_3$) δ 1.23-1.43 (m, 36H), 1.60 (brs, 2H, exchD_2O), 1.69-1.73 (m, 4H), 1.96-1.99 (m, 4H), 2.56-2.59 (m, 4H), 3.23-3.32 (m, 16H), 3.68 (s, 4H), 4.20 (t, 4H, *J* = 6.0 Hz), 7.17 (s, 4H), 8.57 (s, 4H). MS (ESI) *m/z* = 1083 $(M+H)^+$

(31): Yellow oil: 18% yield; ^{1}H NMR (400MHz, $CDCl_3$) δ 1.23-1.43 (m, 36H), 1.78-1.97 (m, 12H), 2.69-2.74 (m, 4H), 3.17-3.31 (m, 16H), 3.80 (s, 4H), 4.20 (t, 4H, *J* = 8.0 Hz), 7.37 (s, 4H), 8.64 (s, 4H). MS (ESI) *m/z* = 1111 $(M+H)^+$

(32): Yellow oil: 34% yield; ^{1}H NMR (400MHz, $CDCl_3$) δ 1.36-1.42 (m, 36H), 1.49-1.57 (m, 8H), 1.81-1.87 (m, 4H), 1.91-1.98 (m, 4H), 2.68-2.71 (m, 4H), 3.14-3.28 (m, 16H), 3.81 (s, 4H), 4.19 (t, 4H, *J* = 6.0 Hz), 7.40 (s, 4H), 8.69 (s, 4H). MS (ESI) *m/z* = 1139 $(M+H)^+$

8) Dihydrochloride salt: Pink solid: 23% yield; mp > 250°C; ^{1}H NMR (400MHz, D_2O) δ 1.15 (m, 8H), 1.87- 1.99 (m, 8H), 3.06-3.15 (m, 8H), 3.27-3.29 (m, 4H), 3.41-3.44 (m, 4H), 3.59 (t, 4H, *J* = 5.4 Hz), 4.22 (s, 4H), 4.22 (t, 4H, *J* = 6.0 Hz) 7.50 (s, 4H), 8.46 (s, 4H); ^{13}C NMR (100MHz, D_2O) δ 25.20, 25.31, 26.78, 39.05, 45.00, 50.06, 67.60, 68.91, 70.03, 125.28, 125.50, 130.44, 131.05, 131.990, 163.27. MS (ESI) *m/z* = 743 $(M+H)^+$. Elemental analysis for $C_{42}H_{54}N_4O_8.2HCl.2H_2O$ Calculated: C, 59.22; H, 7.10; N, 6.58; Found: C, 59.50; H, 7.26; N, 5.85.

General procedure for the synthesis of 4-7.

To a cooled solution (0°C) of the appropriate compound **29-32** (1 eq) in MeOH was added dropwise a solution of 3N HCl. The reaction mixture was stirred overnight at room temperature, then the solvent was removed in vacuo. The residue was taken up with H_2O and washed 3 times with diethyl ether. The aqueous phase was evaporated in vacuo to obtain **4-7**, as hydrochloride salts.

(4): Yellow solid: quantitative yield; mp >250 °C; ^{1}H NMR (400MHz, D_2O) δ 2.03-2.19 (m, 8H), 3.01-3.14 (m, 12H), 4.21 (s, 4H), 4.33 (t, 4H, *J* = 5.8 Hz), 7.43 (s, 4H), 8.50 (s, 4H); ^{13}C NMR (100MHz, D_2O) δ 21.80, 24.07, 37.04, 43.82, 44.17, 50.55, 125.72, 125.83, 130.57, 130.81, 131.17, 164.15; MS (ESI) *m/z* = 597 $(M+H)^+$. Elemental analysis for $C_{35}H_{43}N_6O_4.4HCl.2H_2O$ Calculated: C, 52.97; H, 6.48; N, 10.59; Found: C, 53.12; H, 6.23; N, 10.31.

(5): Yellow solid: quantitative yield; mp >250 °C; ^{1}H NMR (400MHz, D_2O) δ 2.14-2.26 (m, 8H), 3.15-3.27 (m, 12H), 3.50 (m, 8H), 4.30 (s, 4H), 4.35 (t, 4H, *J* = 6.0 Hz), 7.54 (s, 4H), 8.73 (s, 4H); ^{13}C NMR (100MHz, D_2O) δ 22.46, 24.48, 37.43, 42.63, 42.56, 43.45, 44.72, 45.53, 50.33, 125.64, 130.66, 131.14, 131.49, 164.11; MS (ESI) *m/z* = 683 $(M+H)^+$. Elemental analysis for

$C_{38}H_{50}N_8O_4.6HCl.4H_2O$ Calculated: C, 46.87; H, 6.63; N, 11.51; Found: C, 47.01; H, 6.46; N, 10.05.

(6): Yellow solid: quantitative yield; mp >250 °C; ^{1}H NMR (400MHz, D_2O) δ 2.09-2.14 (m, 8H), 2.17-2.22 (m, 4H), 3.13-3.20 (m, 20H), 4.30 (s, 4H), 4.34 (t, 4H, *J* = 6.0 Hz), 7.56 (s, 4H), 8.73 (s, 4H); ^{13}C NMR (100MHz, D_2O) δ 22.36, 24.20, 37.29, 43.6, 44.28, 44.31, 44.42, 45.00, 50.52, 126.15, 126.20, 130.70, 131.12, 131.73, 164.62; MS (ESI) *m/z* = 356 $(M+2H)^{+2}$. Elemental analysis for $C_{40}H_{54}N_8O_4.6HCl.3H_2O$ Calculated: C, 48.84; H, 6.76; N, 11.39; Found: C, 48.75; H, 6.57; N, 10.98.

(7): Yellow solid: 92% yield; mp < 250°C; ^{1}H NMR (400MHz, D_2O) δ 1.76-1.78 (m, 8H), 2.09-2.71 (m, 8H), 3.07-3.16 (m, 20H), 4.28-4.31 (m, 8H), 7.55 (s, 4H), 8.60 (s, 4H); ^{13}C NMR (100MHz, D_2O) δ 21.96, 22.33, 22.46, 24.38, 37.47, 43.54, 44.14, 44.92, 46.51, 50.40, 53.7, 125.96, 130.66, 131.11, 131.08, 164.38; MS (ESI) *m/z* = 370 $(M+2H)^{+2}$. Elemental analysis for $C_{42}H_{58}N_8O_4.6HCl.4H_2O$ Calculated: C, 48.99; H, 7.05; N, 10.88; Found: C, 49.23; H, 7.03; N, 10.61.

Fluorescence Resonance Energy Transfer (FRET)

The following oligonucleotide sequences, all purchased from Eurofins, were used: F21T: (5´- FAM-GGG TTA GGG TTA GGG TTA GGG-TAMRA-3´), c-KIT (5´-FAM-CCC GGG CGG GCG CGA GGG AGG GGA GG-TAMRA-3´), T-Loop: (5´-FAM-TAT AGC TATA TTT TTT TATA GCT ATA-TAMRA-3´). TAMRA (6-carboxytetramethylrhodamine) is the acceptor fluorophore, and FAM (6-carboxyfluorescein) is the donor fluorophore. From 50 µM stock solutions, 400 nM solutions in FRET buffer (60 mM potassium cacodylate pH 7.4) were prepared. The nucleotides were annealed by heating the samples to 90 °C for 10 min and allowing them to cool down to RT within 4 h. 1 mM solutions of the compounds in deionised water were prepared and diluted to double of the required concentrations with FRET buffer. RT-PCR 96 well plates (MJ Research, Waltham, MA) were used. Each well was loaded with 50 µL of nucleotide solution and 50 µL of drug solution. Drug concentrations of 0.1, 0.2, 0.5, 1, 2 and 5 µM were used, and every drug concentration was repeated 3 times. Measurements were made on a DNA Opticon Engine (MJ Research) with excitation at 450 – 495 nm and detection at 515 – 545 nm. The flourescence was read at intervals of 0.5 °C over the range 30 – 100 °C. Before each reading the temperature was held constant for 30 s. The raw data were processed using Origin (Version 7.0, OriginLab Corp.). The graphs were smoothed using a 10-point running average and normalized. The melting temperatures were obtained by determining the maxima of the first derivative of the smooth melting curves. The value ΔT is the melting temperature difference between the nucleotide sequence with drug and the negative control.

Cell Culture

The cell lines MCF7, A549, ALT, PANC-1, MIA-PaCa-2 (European Collection of Cell Cultures) and WI38 (American Type Culture Collection) were maintained in monolayer culture in 75 cm2 flasks (TPP, Switzerland) under a humidified 5 % CO_2 atmosphere at 37°C. For the A549 cell line, Dulbecco's MEM medium (GIBCO 21969, Invitrogen, UK) supplemented with L-glutamine (2 mM, GIBCO 25030, Invitrogen, UK), essential amino acids (1 %, GIBCO 11140, Invitrogen, UK), and foetal calf serum (10 %, S1810, Biosera, UK) was used. For MIA-Pa-Ca-2 and PANC-1, Dulbecco's MEM, supplemented with L-glutamine (2 mM) and foetal calf serum (10 %) was used.

The medium MEM (M2279, Sigma, UK) with added L-glutamine (2 mM), essential amino acids (1 %) and foetal calf serum (10 %) was used for the MCF7, ALT and WI38 cell lines. To passage the cells, they were washed with PBS (GIBCO 14040, Invitrogen, UK), treated with trypsine (GIBCO 25300, Invitrogen, UK), and re-seeded into fresh medium, resulting in an initial cell density of approximately $1x10^4$ cells/mL medium. Cells were counted using a Neubauer haemocytometer (Assistant, Germany) by microscopy or a MacsQuant flow cytometer (Miltenyi Biotech, Germany) on a suspension of cells obtained by washing with PBS, trypsinisation, centrifugation at 8 °C at 8000 rpm for 3 minutes, and re-suspension in fresh medium.

Sulforhodamine B (SRB) short-term cytotoxicity assay

Cells were counted and diluted to the required concentration in 20 mL medium. For the cell lines A549, PANC-1 and MIA-Pa-Ca-2, 2000 cells with 160 µL media were seeded into each well of a 96 well plate (Nunc, Denmark). For WI38, 6000 cells per well, and for ALT and MCF7 4000 cells per well were used due to their greaterdoubling time. After incubation for 24 hours, the compounds to be tested, dissolved in 40 µL of medium, were added at different concentrations, and the cells incubated for 96 hours. The medium was then removed and the cells fixed by incubation with TCA (10 %, Sigma-Aldrich, UK) in water for 30 min. After removal of the TCA, the cells were washed with deionised water 5 times and dried at 60 °C for 1 h. Cells were then incubated with SRB (80 µL, 0.4 % in 1 % acetic acid, Acros Organics, UK) for 15 min at RT. The SRB was removed, the wells washed with 1 % acetic acid (200 µL), and dried at 60 °C for 1 h. Tris-base (100 µL, 10 mM, Acros Organics, UK) solution was added to each well, and the plates were gently shaken for 5 min. The absorbance at 540 nm was measured with a plate reader (Spectrostar Omega, BMG Labtech, Germany). The data were normalised to the value of 100 for the control experiment (untreated cells), and the IC_{50} values were obtained by interpolation from a plot done with Origin (Version 7.0, OriginLab Corp.), as the concentration leading to an absorbance intensity of 50%.

TRAP assay

Telomerase activity was determined using the TRAP-LIG assay,[60] a modified telomere repeat amplification protocol that ensures that there is no carryover of ligand into the second PCR step of the assay.1 µg of protein from untreated and treated cells were incubated with TS forward primer (0.1 µg/µL of 5´-AAT CCG TCG AGC AGA GTT-3´) at 30 ºC for 10min, followed by 94ºC for 5 min and a final maintenance of the mixture at 20 ºC, to allow the initial elongation to take place. Elongated products were purified using the QIAquick nucleotide purification kit (Qiagen) according to the manufacturer's instructions. Eluted samples were redissolved in PCR grade water and subjected to amplification in master mix containing ACX reverse primer (1 µM, 5´-GCG CGG $[CTTACC]_3$ CTA ACC-3´), TS forward primer (0.1 µg), TRAP buffer, BSA (5 µg), 0.5 mM dNTPs, and 2U RedHot Taq polymerase for 35 cycles of 94 ºC for 30 s, 61 ºC for 1 min, and at 72 ºC for 1 min. Samples were separated on a 12% PAGE and visualized with SYBR green staining. Treated samples were normalized against positive control containing protein only and all the samples were corrected for background by subtracting the fluorescence reading of the negative controls.

Acknowledgments

A.M. and C.M. thank Ilaria Gober for excellent technical support. The authors wish to thank Uni.Rimini SpA, University of Bologna (RFO), Italian Ministry of Education (MIUR) FIRB-IDEAS (code FIRB RBID082ATK_003), and PRIN 2009 (code 2009MFRKZ8). Work in the Neidle laboratory has been supported by the Pancreatic Cancer Research Fund and the Medical Research Council.

Figure and Scheme captions

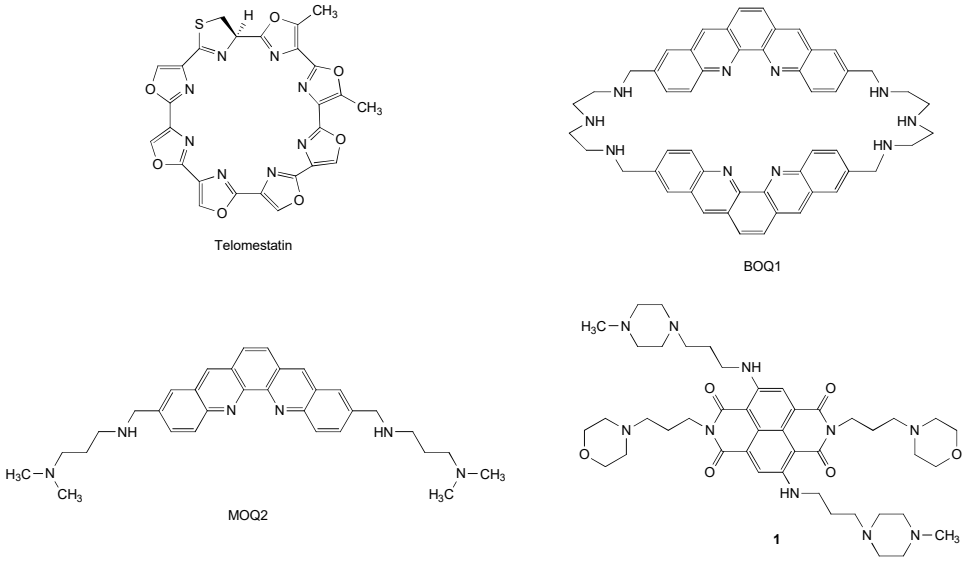

Fig. 1. Selected examples of G-quadruplex binders.

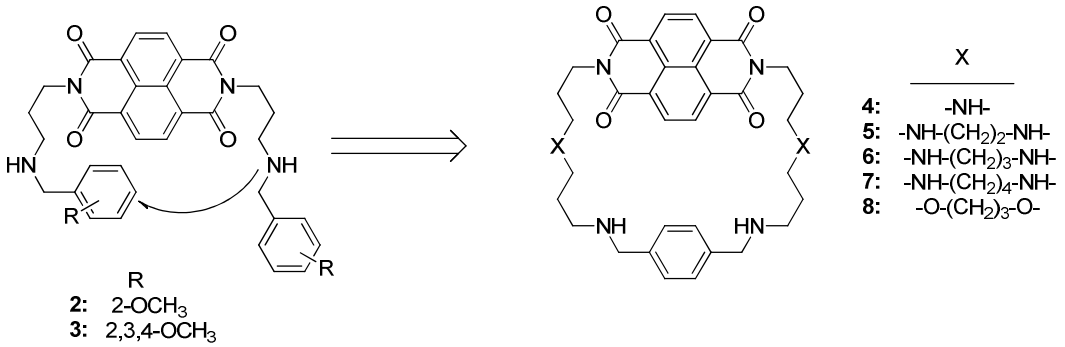

Fig.2. Drug design strategy leading to **4-8**.

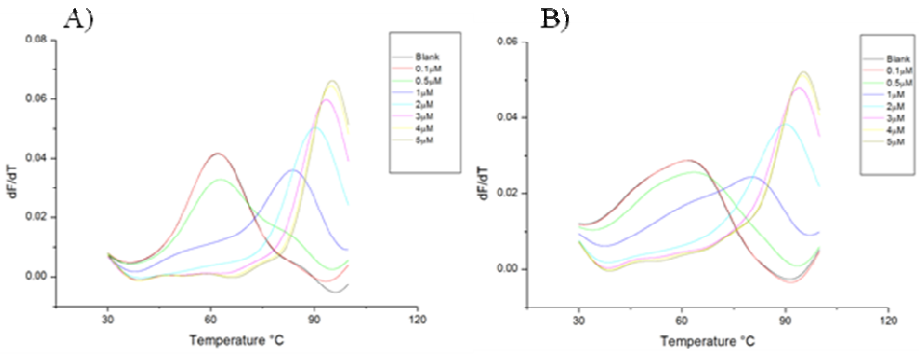

Fig. 3. FRET melting curve for compound **6** at different ligand concentration with A) the h-tel F21T quadruplex sequence and B) the c-KIT promoter quadruplex sequence.

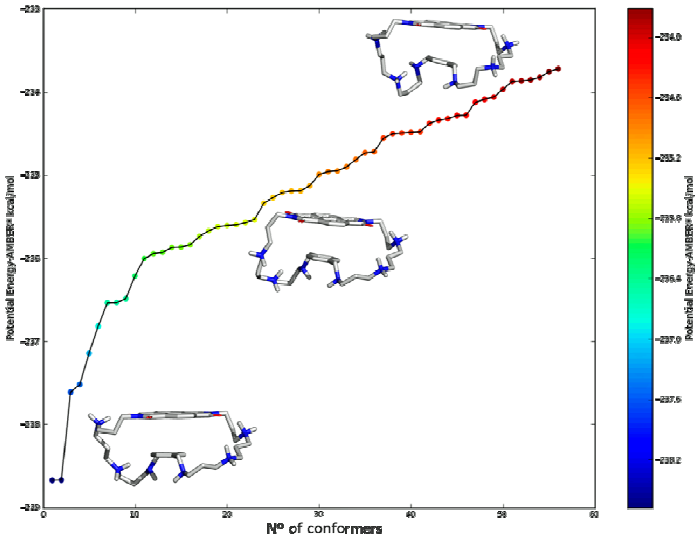

Fig. 4. Potential energy scatter plot of the 56 conformers of compound **6** found in the conformational search. Non polar hydrogen atoms are omitted for clarity.

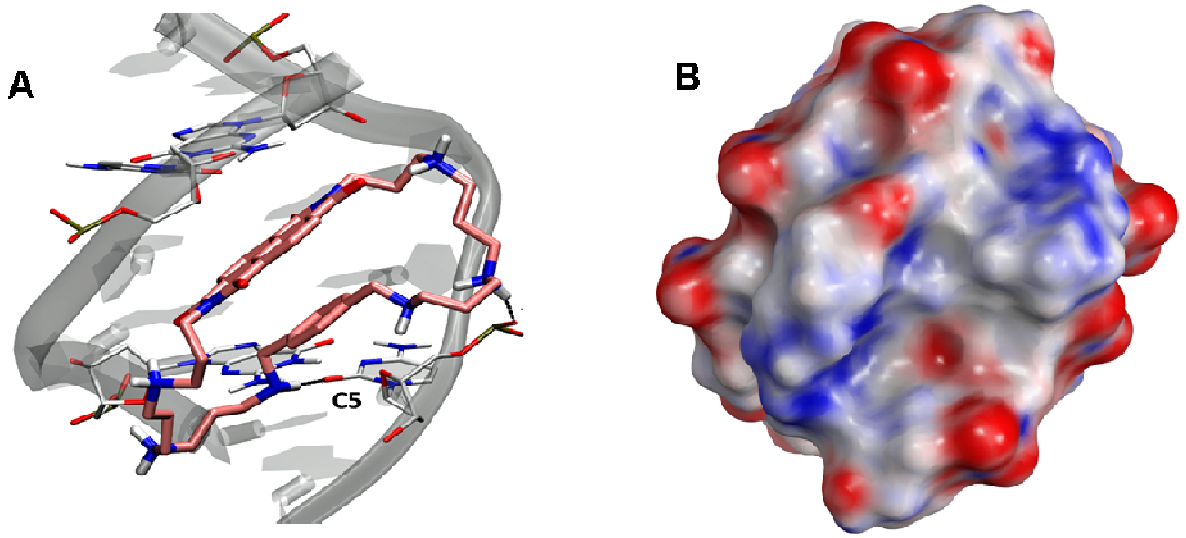

Fig. 5. A) Binding mode of compound **6** against a duplex DNA (PDB entry: 1Z3F) and the hydrogen bond interactions involved. Compound **6** is represented as pink-coloured sticks while the duplex DNA is shown as a transparent gray ribbon. Hydrogen bonds are depicted as dashed black lines. **B)** The Poisson-Boltzmann electrostatic potential surface area computed using Maestro ver. 9.7; red and blue colors are respectively related to negative and positive areas.

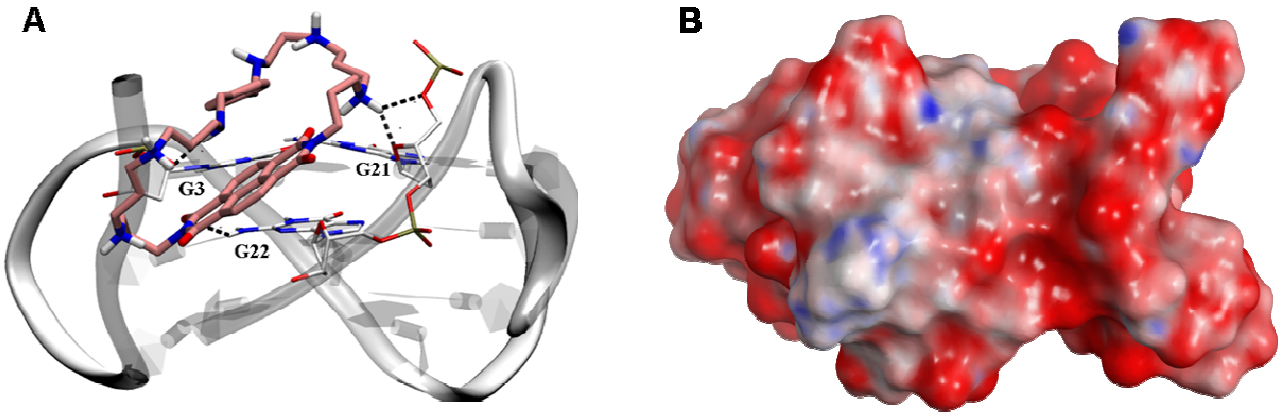

Fig. 6. A) Docking best pose of compound **6** against a human telomeric DNA quadruplex (PDB entry: 3CDM) and the hydrogen bond interactions involved. Compound **6** is in stick represention while the quadruplex DNA is shown as a white ribbon. Hydrogen bonds are depicted as dashed black lines. **B)** The Poisson-Boltzmann electrostatic potential surface area computed using Maestro ver. 9.7.

Table 1. ΔT_m Values (° C) for FRET analyses of compounds **2**, **4-8** at 1 μM with two G-quadruplex sequences: h-Tel (F21T), c-KIT and duplex DNA (T-loop). Esds are triplicate measurements and average 0.3 °C.

Compound	F21T	c-KIT	T-loop

2	9.9	7.4	2.2
4	12.6	12.2	1.4
5	18.9	14.3	1.2
6	22.1	15.1	3.3
7	26.8	33.1	8.6
8	0.4	0	0.2

Table 2. Short-term 96 hr IC_{50} values (in µM) for compounds **2**, **4-8** in a cancer cell line panel, comprising A549 (lung cancer), MCF7 (breast), MIA-PaCa-2 and PANC-1 (pancreatic cancer), ALT (alternative Lengthening of Telomeres) and WI38 (lung fibroblast) cell lines. Esds average 0.25 µM. Values are the mean of triplicate experiments and esds are in the range 0.1-0.3 µM.

Compound	A549	MCF7	MIA-PaCa2	PANC-1	ALT	WI38
2	0.2	0.3	0.2	0.4	0.2	0.4
4	1.0	0.8	0.4	0.4	1.00	1.3
5	5.2	5.5	0.7	1.0	3.3	6.1
6	4.6	19.1	8.6	8.2	>25	>25
7	10.4	>25	19.3	13.6	14.9	>25
8	0.5	1.2	1.0	0.6	1.1	2.9

Table 3: Details on the best pose of **6** against the two DNA targets, with their PDB codes in parentheses. ΔG is the free energy of complexation, *d*Electr. is the electrostatic term, *d*VdW is the van der Waals term and *d*GB/SA is the *d*GB/SA is the Gibbs-Born Surface Area solvation term, all expressed in kcal/mol. H-bonds are the ligand-target number of hydrogen bonds and BP is the percentage best pose Boltzmann's population computed at room temperature with respect to all poses obtained.

Target	ΔG	*d*Electr.	*d*vdW	*d*GB/SA	H-bonds	BP
G-quadruplex (3CDM)	-63.69	-1983.74	-50.59	1970.64	5	98.95
Duplex (1Z3F)	-27.18	-1198.11	-37.72	1208.65	2	100

Scheme 1.

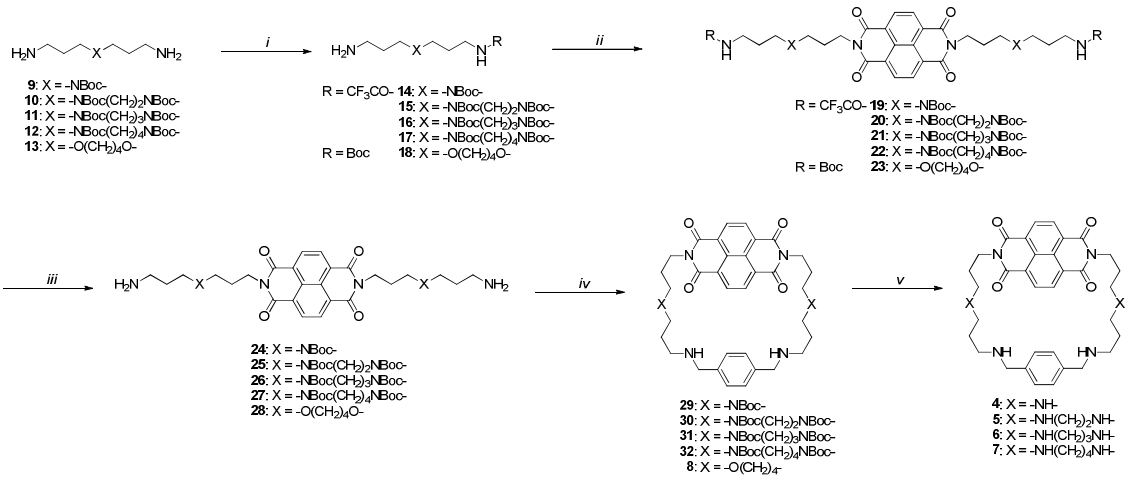

Scheme 1: *i*) for **14-15** CF_3COOEt, MeOH, rt, 12h, 74-95% yields, for **18** Boc_2O, CH_2Cl_2, rt, 12h, 93% yield; *ii*) 1,4,5,8-Naphthalentetracarboxylicdianhydride, DMF, reflux, 2h, 16-90% yields; *iii*) for **24-27** K_2CO_3, H_2O/MeOH, rerflux, 2h, 44-63% yields, for **28** HCl 2N, MeOH, rt, 12h, 88% yield; *iv) a.* terephthalaldehyde, EtOH, rt, 72h, b. $NaBH_4$, rt, 12h, 18-34% yields; v) HCl 3N, MeOH, rt, 12h, quantitative yields

References and notes

1. Hurley, L. H. *Nat Rev Cancer* **2002,** *2*, 188.
2. Bochman, M. L.; Paeschke, K.; Zakian, V. A. *Nat Rev Genet* **2012,** *13*, 770.
3. Balasubramanian, S.; Hurley, L. H.; Neidle, S. *Nat Rev Drug Discov* **2011,** *10*, 261.
4. Phan, A. T. *FEBS J* **2010,** *277*, 1107.
5. Harley, C. B.; Futcher, A. B.; Greider, C. W. *Nature* **1990,** *345*, 458.
6. Autexier, C.; Lue, N. F. *Annu Rev Biochem* **2006,** *75*, 493.
7. Mocellin, S.; Pooley, K. A.; Nitti, D. *Trends Mol Med* **2013,** *19*, 125.
8. Sekaran, V.; Soares, J.; Jarstfer, M. B. *J Med Chem* **2014,** *57*, 521.
9. Brunsvig, P. F.; Aamdal, S.; Gjertsen, M. K.; Kvalheim, G.; Markowski-Grimsrud, C. J.; Sve, I.; Dyrhaug, M.; Trachsel, S.; Møller, M.; Eriksen, J. A.; Gaudernack, G. *Cancer Immunol Immunother* **2006,** *55*, 1553.
10. Herbert, B. S.; Gellert, G. C.; Hochreiter, A.; Pongracz, K.; Wright, W. E.; Zielinska, D.; Chin, A. C.; Harley, C. B.; Shay, J. W.; Gryaznov, S. M. *Oncogene* **2005,** *24*, 5262.
11. El-Daly, H.; Kull, M.; Zimmermann, S.; Pantic, M.; Waller, C. F.; Martens, U. M. *Blood* **2005,** *105*, 1742.
12. Ruden, M.; Puri, N. *Cancer Treat Rev* **2013,** *39*, 444.
13. Williams, S. C. *Nat Med* **2013,** *19*, 6.
14. Shay, J. W.; Reddel, R. R.; Wright, W. E. *Science* **2012,** *336*, 1388.
15. Zahler, A. M.; Williamson, J. R.; Cech, T. R.; Prescott, D. M. *Nature* **1991,** *350*, 718.
16. Sun, D.; Thompson, B.; Cathers, B. E.; Salazar, M.; Kerwin, S. M.; Trent, J. O.; Jenkins, T. C.; Neidle, S.; Hurley, L. H. *J Med Chem* **1997,** *40*, 2113.
17. Biffi, G.; Tannahill, D.; McCafferty, J.; Balasubramanian, S. *Nat Chem* **2013,** *5*, 182.
18. Hsu, S. T.; Varnai, P.; Bugaut, A.; Reszka, A. P.; Neidle, S.; Balasubramanian, S. *J Am Chem Soc* **2009,** *131*, 13399.
19. Phan, A. T.; Modi, Y. S.; Patel, D. J. *J Am Chem Soc* **2004,** *126*, 8710.
20. Cogoi, S.; Xodo, L. E. *Nucleic Acids Res* **2006,** *34*, 2536.
21. Sun, D.; Liu, W. J.; Guo, K.; Rusche, J. J.; Ebbinghaus, S.; Gokhale, V.; Hurley, L. H. *Mol Cancer Ther* **2008,** *7*, 880.
22. Palumbo, S. L.; Ebbinghaus, S. W.; Hurley, L. H. *J Am Chem Soc* **2009,** *131*, 10878.

23. Riou, J. F.; Guittat, L.; Mailliet, P.; Laoui, A.; Renou, E.; Petitgenet, O.; Mégnin-Chanet, F.; Hélène, C.; Mergny, J. L. *Proc Natl Acad Sci U S A* **2002,** *99*, 2672.
24. Balasubramanian, S.; Neidle, S. *Curr Opin Chem Biol* **2009,** *13*, 345.
25. Neidle, S. *FEBS J* **2010,** *277*, 1118.
26. Ohnmacht, S. A.; Neidle, S. *Bioorg Med Chem Lett* **2014,** *24*, 2602.
27. Drygin, D.; Siddiqui-Jain, A.; O'Brien, S.; Schwaebe, M.; Lin, A.; Bliesath, J.; Ho, C. B.; Proffitt, C.; Trent, K.; Whitten, J. P.; Lim, J. K.; Von Hoff, D.; Anderes, K.; Rice, W. G. *Cancer Res* **2009,** *69*, 7653.
28. Shin-ya, K.; Wierzba, K.; Matsuo, K.; Ohtani, T.; Yamada, Y.; Furihata, K.; Hayakawa, Y.; Seto, H. *J Am Chem Soc* **2001,** *123*, 1262.
29. Miyazaki, T.; Pan, Y.; Joshi, K.; Purohit, D.; Hu, B.; Demir, H.; Mazumder, S.; Okabe, S.; Yamori, T.; Viapiano, M.; Shin-ya, K.; Seimiya, H.; Nakano, I. *Clin Cancer Res* **2012,** *18*, 1268.
30. Teulade-Fichou, M. P.; Carrasco, C.; Guittat, L.; Bailly, C.; Alberti, P.; Mergny, J. L.; David, A.; Lehn, J. M.; Wilson, W. D. *J Am Chem Soc* **2003,** *125*, 4732.
31. Collie, G. W.; Promontorio, R.; Hampel, S. M.; Micco, M.; Neidle, S.; Parkinson, G. N. *J Am Chem Soc* **2012,** *134*, 2723.
32. Micco, M.; Collie, G. W.; Dale, A. G.; Ohnmacht, S. A.; Pazitna, I.; Gunaratnam, M.; Reszka, A. P.; Neidle, S. *J Med Chem* **2013,** *56*, 2959.
33. Tumiatti, V.; Milelli, A.; Minarini, A.; Micco, M.; Gasperi Campani, A.; Roncuzzi, L.; Baiocchi, D.; Marinello, J.; Capranico, G.; Zini, M.; Stefanelli, C.; Melchiorre, C. *J Med Chem* **2009,** *52*, 7873.
34. Milelli, A.; Tumiatti, V.; Micco, M.; Rosini, M.; Zuccari, G.; Raffaghello, L.; Bianchi, G.; Pistoia, V.; Fernando Díaz, J.; Pera, B.; Trigili, C.; Barasoain, I.; Musetti, C.; Toniolo, M.; Sissi, C.; Alcaro, S.; Moraca, F.; Zini, M.; Stefanelli, C.; Minarini, A. *Eur J Med Chem* **2012,** *57*, 417.
35. Parise, A.; Milelli, A.; Tumiatti, V.; Minarini, A.; Neviani, P.; Zuccari, G. *Drug Deliv* **2013**.
36. Driggers, E. M.; Hale, S. P.; Lee, J.; Terrett, N. K. *Nat Rev Drug Discov* **2008,** *7*, 608.
37. Micheli, E.; Lombardo, C. M.; D'Ambrosio, D.; Franceschin, M.; Neidle, S.; Savino, M. *Bioorg Med Chem Lett* **2009,** *19*, 3903.
38. Czerwinska, I.; Sato, S.; Juskowiak, B.; Takenaka, S. *Bioorg Med Chem* **2014,** *22*, 2593.
39. Esaki, Y.; Islam, M. M.; Fujii, S.; Sato, S.; Takenaka, S. *Chem Commun (Camb)* **2014,** *50*, 5967.
40. Wellendorph, P.; Jaroszewski, J. W.; Hansen, S. H.; Franzyk, H. *Eur J Med Chem* **2003,** *38*, 117.
41. Rankin, S.; Reszka, A. P.; Huppert, J.; Zloh, M.; Parkinson, G. N.; Todd, A. K.; Ladame, S.; Balasubramanian, S.; Neidle, S. *J Am Chem Soc* **2005,** *127*, 10584.
42. Gunaratnam, M.; Swank, S.; Haider, S. M.; Galesa, K.; Reszka, A. P.; Beltran, M.; Cuenca, F.; Fletcher, J. A.; Neidle, S. *J Med Chem* **2009,** *52*, 3774.
43. Mitchell, J. L.; Thane, T. K.; Sequeira, J. M.; Thokala, R. *Biochem Soc Trans* **2007,** *35*, 318.
44. Seiler, N.; Delcros, J. G.; Moulinoux, J. P. *Int J Biochem Cell Biol* **1996,** *28*, 843.
45. Minarini, A.; Milelli, A.; Tumiatti, V.; Rosini, M.; Bolognesi, M. L.; Melchiorre, C. *Amino Acids* **2010,** *38*, 383.
46. Emanuela, B.; Minarini, A.; Tumiatti, V.; Milelli, A.; Lunelli, M.; Pegoraro, M.; Rizzoli, V.; Di Paolo, M. L. *Amino Acids* **2012,** *42*, 913.
47. Saiki, R.; Yoshizawa, Y.; Minarini, A.; Milelli, A.; Marchetti, C.; Tumiatti, V.; Toida, T.; Kashiwagi, K.; Igarashi, K. *Bioorg Med Chem Lett* **2013,** *23*, 3901.
48. Minarini, A.; Zini, M.; Milelli, A.; Tumiatti, V.; Marchetti, C.; Nicolini, B.; Falconi, M.; Farruggia, G.; Cappadone, C.; Stefanelli, C. *Eur J Med Chem* **2013,** *67*, 359.
49. Senanayake, M. D.; Amunugama, H.; Boncher, T. D.; Casero, R. A.; Woster, P. M. *Essays Biochem* **2009,** *46*, 77.
50. Liang, F.; Wan, S. H.; Li, Z.; Xiong, X. Q.; Yang, L.; Zhou, X.; Wu, C. T. *Current Medicinal Chemistry* **2006,** *13*, 711.
51. Canals, A.; Purciolas, M.; Aymamí, J.; Coll, M. *Acta Crystallogr D Biol Crystallogr* **2005,** *61*, 1009.
52. Parkinson, G. N.; Cuenca, F.; Neidle, S. *J Mol Biol* **2008,** *381*, 1145.
53. Schrödinger Release 2014-1: Maestro, version 9.7, Schrödinger, LLC, New York, NY, 2014
54. Schrödinger Release 2014-1: LigPrep, version 2.9, Schrödinger, LLC, New York, NY, 2014
55. Alcaro, S.; Artese, A.; Costa, G.; Distinto, S.; Ortuso, F.; Parrotta, L. *Biochimie* **2011,** *93*, 1267.
56. Doria, F.; Nadai, M.; Folini, M.; Di Antonio, M.; Germani, L.; Percivalle, C.; Sissi, C.; Zaffaroni, N.; Alcaro, S.; Artese, A.; Richter, S. N.; Freccero, M. *Org Biomol Chem* **2012,** *10*, 2798.
57. Polak, E.; Ribiere, G.; Rev. Fr. Inf. Rech. Oper., 1969; Vol. 16, 35.

58. Morris, G. M.; Huey, R.; Lindstrom, W.; Sanner, M. F.; Belew, R. K.; Goodsell, D. S.; Olson, A. J. *J Comput Chem* **2009,** *30*, 2785.
59. Artese, A.; Costa, G.; Distinto, S.; Moraca, F.; Ortuso, F.; Parrotta, L.; Alcaro, S. *Eur J Med Chem* **2013,** *68*, 139.
60. Reed, J.; Gunaratnam, M.; Beltran, M.; Reszka, A. P.; Vilar, R.; Neidle, S. *Anal Biochem* **2008,** *380*, 99.